

Super-sensitivity measurement of tiny Doppler frequency shifts based on parametric amplification and squeezed vacuum state

Zhi-Yuan Wang(王志远), Zi-Jing Zhang(张子静), and Yuan Zhao(赵远)
Citation: Chin. Phys. B, 2021, 30 (**7**): 074202. DOI: 10.1088/1674-1056/abe3e5
Journal homepage: http://cpb.iphy.ac.cn; http://iopscience.iop.org/cpb

What follows is a list of articles you may be interested in

Optical enhanced interferometry with two-mode squeezed twin-Fock states and parity detection

Li-Li Hou(侯丽丽), Shuai Wang(王帅), Xue-Fen Xu(许雪芬)
Chin. Phys. B, 2020, 29 (**3**): 034203. DOI: 10.1088/1674-1056/ab6837

Quantum optical interferometry via general photon-subtracted two-mode squeezed states

Li-Li Hou(侯丽丽), Jian-Zhong Xue(薛建忠), Yong-Xing Sui(眭永兴), Shuai Wang(王帅)
Chin. Phys. B, 2019, 28 (**9**): 094217. DOI: 10.1088/1674-1056/ab38a9

Quantum interferometry via a coherent state mixed with a squeezed number state

Li-Li Hou(侯丽丽), Yong-Xing Sui(眭永兴), Shuai Wang(王帅), Xue-Fen Xu(许雪芬)
Chin. Phys. B, 2019, 28 (**4**): 044203. DOI: 10.1088/1674-1056/28/4/044203

Phase estimation of phase shifts in two arms for an SU(1,1) interferometer with coherent and squeezed vacuum states

Qian-Kun Gong(龚乾坤), Dong Li(李栋), Chun-Hua Yuan(袁春华), Ze-Yu Qu(区泽宇), Wei-Ping Zhang(张卫平)
Chin. Phys. B, 2017, 26 (**9**): 094205. DOI: 10.1088/1674-1056/26/9/094205

Super-resolution and super-sensitivity of entangled squeezed vacuum state using optimal detection strategy

Jiandong Zhang(张建东), Zijing Zhang(张子静), Longzhu Cen(岑龙柱), Shuo Li(李硕), Yuan Zhao(赵远), Feng Wang(王峰)
Chin. Phys. B, 2017, 26 (**9**): 094204. DOI: 10.1088/1674-1056/26/9/094204

Super-sensitivity measurement of tiny Doppler frequency shifts based on parametric amplification and squeezed vacuum state

Zhi-Yuan Wang(王志远), Zi-Jing Zhang(张子静)[†], and Yuan Zhao(赵远)[‡]

Department of Physics, Harbin Institute of Technology, Harbin 150001, *China*

(Received 2 December 2020; revised manuscript received 19 January 2021; accepted manuscript online 7 February 2021)

The precision measurement of Doppler frequency shifts is of great significance for improving the precision of speed measurement. This paper proposes a precision measurement scheme of tiny Doppler shifts by a parametric amplification process and squeezed vacuum state. This scheme takes a parametric amplification process and squeezed vacuum state into a detection system, so that the measurement precision of tiny Doppler shifts can exceed the Cramér–Rao bound of coherent light. Simultaneously, a simulation study is carried out on the theoretical basis, and the following results are obtained: for the signal light of Gaussian mode, when the amplification factor $g = 1$ and the squeezed factor $r = 0.5$, the measurement error of Doppler frequency shifts is 14.4% of the Cramér–Rao bound of the coherent light in our system. At the same time, when the local light mode and squeezed vacuum state mode are optimized, the measurement precision of this scheme can be further improved by $\sqrt{(2n+1)/(n+1)}$ times, where n is the mode-order of the signal light.

Keywords: squeezed vacuum state, quantum metrology

PACS: 42.50.–p, 42.50.St **DOI:** 10.1088/1674-1056/abe3e5

1. Introduction

Making use of Doppler frequency shifts to measure speed is very important in many applications.[1–4] The measurement precision of Doppler frequency shifts determines the measurement precision of speed. At present, the methods to improve measurement precision are mainly in two aspects: the first is to use non-classical light sources to improve measurement precision, including the precision measurement of phase,[5–10] the measurement of small beam deflection,[11–13] the measurement of gravitational waves,[14–16] and the precise measurement of the magnetic field,[17] and the second is to use a suitable measurement scheme at the receiving end. For example, Fabre *et al.*[18] gave the standard quantum limit of beam splitting detection when measuring a small beam deflection. Trep *et al.*[19] used a four-quadrant detector combined with a squeezed light source to measure the transversal displacement beyond shot noise limit. Then they adopted a balanced homodyne detection scheme to reach the Cramér–Rao bound of information parameters in optical image. Hsu *et al.*[20] and Delaubert *et al.*[21] found that balanced homodyne detection was the optimal detection scheme for transversal displacement and the tilt measurement, and proved their theoretical scheme in experiment.

The precision measurement of Doppler frequency shifts also occupies an important position in quantum precision measurement. Viza *et al.*[22] used coherent light source and adopted a weak measurement scheme to precisely measure Doppler frequency shifts. Pinel *et al.*[23] used a weak measurement scheme to accurately measure the frequency modulation range of continuous wave. However, the coherent state belongs to a classical light source. No matter how the detection scheme is optimized, there is an unbreakable quantum Cramér–Rao bound for the measurement precision. The emergence of quantum state light sources and the maturity of non-linear technology make it possible to break through the Cramér–Rao bound of coherent light measurement, and to further improve the measurement precision of Doppler frequency shifts.

This paper incorporates a parametric amplification technique and squeezed vacuum state into the detection system of tiny Doppler frequency shifts, and proposes a theoretical measurement scheme of Doppler frequency shifts. For weak signal detection at long distance, the use of parametric amplification is of importance for improving the measurement precision. The scheme adopts the structure of Michelson interferometer to realize the homodyne detection of local light and signal light. Our research finds that when the n-order $(n > 0)$ Hermite Gaussian beam is adopted as the signal light, the Doppler measurement precision can be improved, and the measurement precision of the system can exceed the Cramér–Rao bound of coherent light through a parametric amplification process and squeezed vacuum state injected. Then we discuss factors influencing the measurement precision in our scheme.

The rest of this paper is organized as follows. In Section 2, the parametric amplification and squeezed vacuum state are used to precisely measure Doppler frequency shifts. In Section 3, the factors influencing tiny Doppler measurement precision are analyzed. In Section 4, some conclusions are drawn from the present study, and the perspectives are also presented, finally.

[†]Corresponding author. E-mail: zhangzijing@hit.edu.cn

[‡]Corresponding author. E-mail: zhaoyuan@hit.edu.cn

© 2021 Chinese Physical Society and IOP Publishing Ltd

2. Using parametric amplification and squeezed vacuum state to precisely measure Doppler frequency shifts

As shown in Fig. 1, we use a beam splitter BS1 (50:50) to divide the laser into local light and signal light. After the signal light passes through an acousto-optic modulator (AOM), its frequency is ω_2, and then the signal light passes through an atomic pool that performs a parametric amplification process to achieve stimulated Raman scattering (SRS). At this time, the signal light is the Stokes seed light in the SRS process. After exiting from the atomic pool, the intensity of signal light will increase.

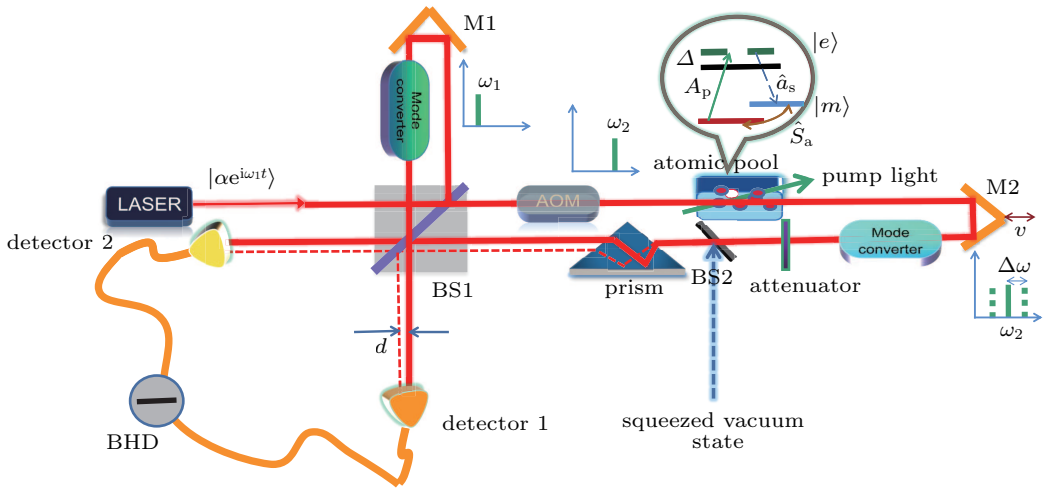


Fig. 1. Doppler precision measurement scheme of parametric amplification and squeezed vacuum state. The laser is divided into the local light and signal light by a beam splitter BS1. The signal light passes through an acousto-optic modulator (AOM) to obtain a frequency shift. The mirror M2 moves at a tiny constant speed, and the signal light is amplified by a parametric amplification process. After the squeezed vacuum state is injected, the signal light is incident on a dispersive prism. This process converts the tiny frequency shifts into the transversal displacements of the beam. The local light that is reflected by mirror M1 and the signal light separately pass through a mode converter, which can change their transversal modes. Finally, the transversal displacement d is obtained by balanced homodyne detection (BHD), and then the tiny Doppler frequency shift $\Delta\omega$ can be obtained.

The Hamiltonian of the interaction among signal light, pump light, and atoms is expressed as $\hat{H} = \mathrm{i}\hbar\eta A_\mathrm{p}\hat{a}_\mathrm{s}^{+}\hat{S}_\mathrm{a}^{+} + \mathrm{h.c.}$, where $\eta = g_\mathrm{em}g_\mathrm{eg}/\Delta$, g_eg is the coupling coefficient between the excited state and the ground state of atoms, and g_em is the coupling coefficient between the excited state and the metastable state, Δ is a detuning parameter between the pump light and the excited state, A_p is the amplitude of pump light. The frequency of the pump light and the frequency of the signal light must satisfy $\omega_\mathrm{P} - \omega_2 = \omega_\mathrm{mg}$, where ω_mg is the energy difference between the ground state and the excited state of atoms. Then the relationship between the input and output of signal light in SRS is

$$\begin{aligned}\hat{a}_\mathrm{s} &= \hat{a}_\mathrm{s0}\cosh g + \hat{S}_\mathrm{a0}^{+}\sinh g,\\ \hat{S}_\mathrm{a} &= \hat{S}_\mathrm{a0}\cosh g + \hat{a}_\mathrm{s0}^{+}\sinh g.\end{aligned} \tag{1}$$

In the above equation, $\hat{a}_\mathrm{s}$ and $\hat{a}_\mathrm{s0}$ are respectively the annihilation operators of the output signal and the input signal, $\hat{S}_\mathrm{a}$ is the atomic spin wave after the signal light has been input into the atomic pool, $\hat{S}_\mathrm{a0}$ is the atomic spin wave before the signal light is input into the atomic pool, and g is a amplification factor in the parametric amplification process. After the signal light interacts with atoms, the photon number N of signal light satisfies $N = \langle\hat{a}_\mathrm{s}^{+}\hat{a}_\mathrm{s}\rangle = N_2\cosh^2 g$ at this time, where N_2 is the photon number of the signal light before parametric amplification. After completing the parametric amplification process, the signal light is reflected by a micro-moving mirror M_2 to produce a tiny Doppler frequency shift, and then we inject the squeezed vacuum state into the signal light through the beam splitter BS2. Finally, the signal light passes through a prism with equal base angles γ and a base length L. The refractive index of the prism satisfies the Cauchy dispersion formula $n(\omega) = A + B\omega^2/(2c\pi)^2 + C\omega^4/(2c\pi)^4$, where A, B, and C are three different Cauchy dispersion coefficients, which are different for different media. ω is the angular frequency of light, and c is the speed of light. When neither the parametric amplification nor squeezed vacuum state is applied, we adopt a balanced homodyne detection (BHD) to detect the signal light. The photon number difference is described by the formula $\hat{n}_- = 2\sqrt{N_1N_2}\times\cos\left((\omega_1 - \omega_2 \pm \Delta\omega)t + \phi_0\right) + \sqrt{N_1}\delta\hat{X}_2^{+}$ (as shown in Eq. (A6) in Appendix A). In this formula, N_1 and N_2 are respectively the photon number of the local light and signal light without parametric amplification, $\delta\hat{X}_2^{+}$ is the quadrature amplitude component of the signal light, ϕ_0 is the initial phase difference between the local light and the signal light. It can be seen from the above formula that when $(\omega_1 - \omega_2 \pm \Delta\omega)t + \phi_0 = 2k\pi$ (k is a positive integer), what is measured by the balanced homodyne detection is the quadrature amplitude noise of the signal light. After considering that the mirror M_2 moves at a constant speed v, a tiny Doppler frequency shift generated by the micro-movement of the mirror M_2 is converted into the transversal displacement d

of the signal beam by a prism. The relationship between the tiny Doppler frequency shift $\Delta\omega$ and the transversal displacement d is described by the following equation:

$$d = \Delta\omega / D, \tag{2}$$

where

$$D = \frac{\left(n^2(\omega) - \cos^2\gamma\right)^{3/2}}{n(\omega) L \sin^2\gamma \cos\gamma \left(2B\omega/(2c\pi)^2 + 4C\omega^3/(2c\pi)^4\right)}. \tag{3}$$

Equation (2) gives the relationship between the value of Doppler frequency shift and the value of transversal displacement, and more importantly, it also gives the relationship between the minimum measurable frequency shift $\Delta\omega_{\min}^{\mathrm{BHD}}$ and the minimum measurable transversal displacement $d_{\min}^{\mathrm{BHD}}$ of the system, that is, $d_{\min}^{\mathrm{BHD}} = \Delta\omega_{\min}^{\mathrm{BHD}}/D$. It is worth mentioning that the minimum measurable displacement $d_{\min}^{\mathrm{BHD}}$of the system is equivalent to the measurement error of the displacement d. Similarly, the minimum measurable frequency shift $\Delta\omega_{\min}^{\mathrm{BHD}}$ of the system is equivalent to the measurement error of the Doppler frequency shift $\Delta\omega$. If we choose the TEM_{n0} mode as the signal light, the mode of the local light should be an $(n+1)$-order mode for extracting the transversal displacement d. Then the positive frequency expressions of the local light and the signal light can be obtained (as shown in Eqs. (B4) and (B5) in Appendix B). After adopting parametric amplification and squeezed vacuum state, the photon number difference detected by the two detectors is

$$\hat{n}_- = \sqrt{N_1}\left(2\sqrt{n+1}\sqrt{\eta N_2 \cosh^2 g}\frac{d}{w_0} + \delta\hat{X}_2^+\right). \tag{4}$$

In the above equation, η is the loss caused by a attenuator and various non-ideal factors, and w_0 is the waist radius of the signal light. We adjust the attenuator at the signal light path to satisfy $N_1 \gg N_2$. The quadrature component fluctuation $\delta\hat{X}_2^+$ of the signal light can be given as $\langle\delta^2\hat{X}_2^+\rangle = \cosh^2 r + \sinh^2 r - 2\sinh r\cosh r\cos\phi$, with r being a squeezed factor and ϕ being the phase difference between signal light and local light. We can give the expression of the signal-to-noise ratio (SNR) after the squeezed vacuum state has been injected as follows:

$$\mathrm{SNR} = \frac{\langle\hat{n}_-\rangle^2}{\langle\Delta^2\hat{n}_-\rangle} = \frac{\left(2\sqrt{n+1}\sqrt{\eta\cosh^2 g N_2}d\right)^2\langle\delta^2\hat{X}_2^+\rangle}{w_0^2}. \tag{5}$$

Figure 2 shows the minimum frequency shift that our system can measure when the phase difference ϕ between signal light and local light is different. As shown in Fig. 2(a), in order to obtain the smallest error of Doppler frequency shift, the phase difference ϕ must be locked at $2k\pi$. When the SNR of the system is equal to 1 and the phase difference is maintained at $2k\pi$, the minimum transversal displacement $d_{\min}^{\mathrm{BHD}}$ and the minimum measurable frequency shift $\Delta\omega_{\min}^{\mathrm{BHD}}$ can be given as follows:

$$d_{\min}^{\mathrm{BHD}} = \frac{w_0 \mathrm{e}^{-r}}{2\sqrt{n+1}\sqrt{\eta N_2 \cosh^2 g}}, \tag{6}$$

$$\Delta\omega_{\min}^{\mathrm{BHD}} = D \cdot \frac{w_0 \mathrm{e}^{-r}}{2\sqrt{n+1}\sqrt{\eta N_2 \cosh^2 g}}. \tag{7}$$

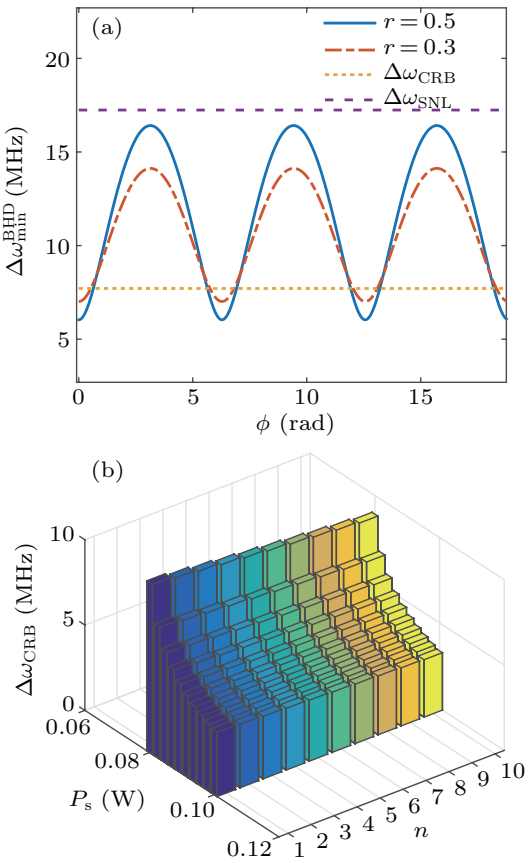


Fig. 2. (a) Relationship between phase difference between signal light and local light and the measurement error of frequency shifts, with parameter amplification factor $g = 0$. When the value of ϕ is $2k\pi$, the measurement error of the system has a minimum value, which can break through the Cramér–Rao bound of coherent light measurement. (b) Relationship among signal light power, signal light order and Cramér–Rao bound of coherent light $\Delta\omega_{\mathrm{CRB}}$, showing that Cramér–Rao bound of coherent light decreases as signal light power increases. At the same time, high-order signal light has higher measurement precision.

The expression of the photon number of signal light in Eq. (6) is $N_2 = P_{\mathrm{s}}\lambda/(hc\cdot\mathrm{RBW})$, where P_{s} is the power of the signal light, h is the Planck constant, RBW is the resolution bandwidth, and λ is the signal light wavelength. The measurement error of Doppler frequency shifts given by the quantum Cramér–Rao bound of coherent light (without adopting parametric amplification and squeezed vacuum state) is $\Delta\omega_{\mathrm{CRB}} = Dw_0/\left(2\sqrt{2n+1}\sqrt{\eta N_2}\right)$ (as shown in Appendix C). Figure 2(b) shows that the larger the number of signal photons and the higher the mode order, the smaller the Cramér–Rao bound of coherent light is. In particular, when $n = 0$, the measurement error of Doppler frequency shifts is defined as the shot noise limit $\Delta\omega_{\mathrm{SNL}}$.

3. Analysis of factors influencing tiny Doppler measurement precision

In Section 2, we have obtained the value of the transversal displacement d from Eq. (4), and the value of the Doppler frequency shift $\Delta\omega$. In this section, we will prove that the precision of our scheme is better than the one with coherent light. We analyze the factors of influencing the Doppler measurement precision, such as the amplification factor and the squeezed factor. At the same time, the modes of local light and squeezed vacuum state can also influence the measurement precision of tiny Doppler frequency shift in our system.

3.1. Influence of amplification factor and squeezed factor on measurement precision

It can be seen from Eq. (6) that when the transversal mode order of the signal light is larger, the measurement error of tiny Doppler frequency shift is smaller. As the squeezed factor r and parametric amplification factor g in this system increase, the minimum measurable frequency shift of the system decreases (as shown in Fig. 3(a)). When both the parametric amplification factor and the squeezed factor are 0, the measurement precision of the system at this time cannot exceed the Cramér–Rao bound of coherent light. After adopting the parametric amplification and squeezed vacuum state injection, the measurement precision of the system breaks through the Cramér–Rao bound of coherent light (as shown in Fig. 3(b)). It verifies the superiority of frequency shift measurement after the parametric amplification and the squeezed vacuum state have been combined. Figure 3(b) shows that for the signal light in Gaussian mode, when the amplification factor $g = 1$ and the squeezed factor $r = 0.5$, the measurement error of Doppler frequency shifts is 14.4% of the error determined by the Cramér–Rao bound of coherent light. With the increase of the signal light order, the measurement error and $\Delta\omega_{\mathrm{CRB}}$decrease. It is shown in Fig. 3(b) that the measurement errors of Doppler frequency shifts are 17.7% and 18.7% of the Cramér–Rao bound of coherent light, when $n = 1$ and 2, respectively. At the same time, as the photon number of signal light increases, our solution can always break through the shot noise limit and the Cramér–Rao bound of coherent light (as shown in Fig. 3(c)).

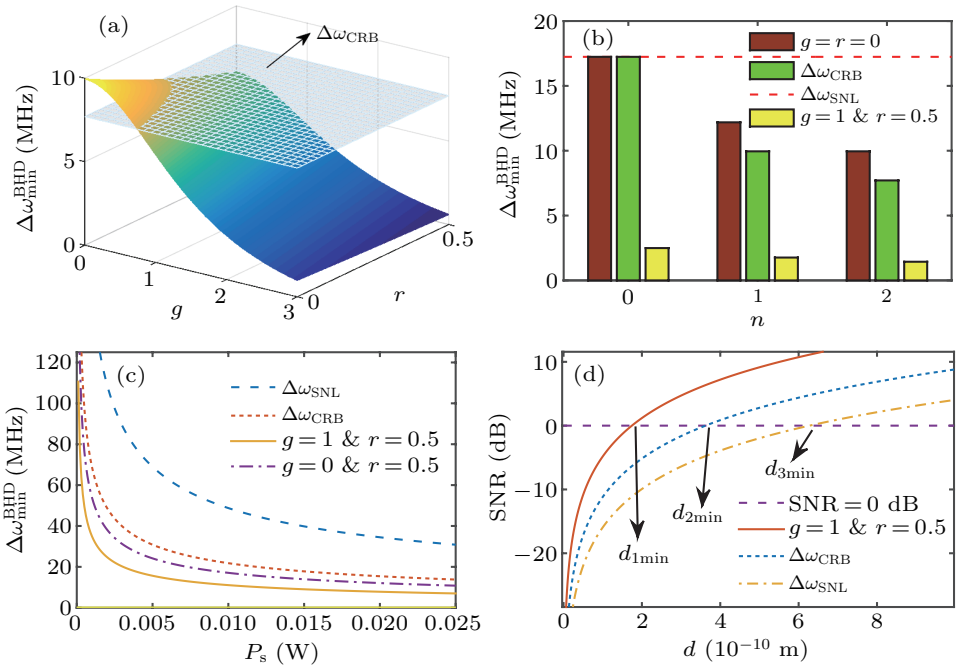


Fig. 3. (a) Relationship among measurement precisions of tiny Doppler frequency shifts, squeezed factor r and parametric amplification factor g, $n = 2$, showing that larger amplification factor and larger squeezed factor will reduce measurement error of the system. (b) Diagram of the measurement error $\Delta\omega_{\mathrm{min}}^{\mathrm{BHD}}$ for different values of amplification factor g and squeezed factor r, indicating that when we choose $g = 1$ and $r = 0.5$, for the signal light in the same order, the measurement precision can exceed the Cramér–Rao bound of coherent light measurement. (c) Functional diagram of $\Delta\omega_{\mathrm{min}}^{\mathrm{BHD}}$ and signal light power. As the signal light power increases, the measurement error of the system will decrease. (d) Relationship between the minimum measurable displacement d of and the SNR of the detection system. When SNR = 1 dB (or SNR = 0 dB), we can obtain the minimum detectable transversal displacement d of the system. So we can obtain $d_{1\,\mathrm{min}} < d_{2\,\mathrm{min}} < d_{3\,\mathrm{min}}$ in Fig. 3(d). It can be seen that the measurement error of the system will be lower than the Cramér–Rao bound of coherent light when using parametric amplification and squeezed vacuum state.

Figure 3(d) shows that the minimum measurable displacement of the system is determined when the SNR is equal to 1. It can be seen from Eq. (2) that the smallest measurable displacement determines the minimum measurable frequency shift of the system. When we adopt parametric amplification and squeezed vacuum state injection, the SNR of the system is improved, and the measurable displacement is reduced. At this time, the measurement precision of the system is improved. The relevant simulation parameters in this paper are $\lambda = 1064$ nm, $w_0 = 53$ μm, the relevant parameters

of the dispersive prism in our system are as follows: $A = 1.60$, $B = 7881\ \mathrm{nm}^{-2}$, $C = 1.7 \times 10^8\ \mathrm{nm}^{-4}$, base angle $\gamma = 15°$, base side length $L = 50$ cm, loss rate $\eta = 96\%$, and resolution bandwidth RBW $= 0.3$ kHz.

3.2. Influence of mode of local light on measurement precision

According to Eq. (A5) in Appendix A, it can be seen that when the signal light in n-order mode is displaced, the components of the $(n-1)$-order mode and $(n+1)$-order mode will be excited. Therefore, for the local light the superposition mode of $(n-1)$-order and $(n+1)$-order is also adopted at this time. It will maximize the SNR and the measurement precision. In order to discuss the mode of local light that makes the detection system have the greatest precision, we set the mode of local light to be $u_2(x) = ru_{n-1}(x) + t\,\mathrm{e}^{\mathrm{i}\phi}u_{n+1}(x)$, where r and t are the weight of the $(n-1)$-mode and $(n+1)$-mode in the local light, satisfying $r^2 + t^2 = 1$, and ϕ is the phase difference between $(n+1)$-order mode and $(n-1)$-order mode. At this time, we can obtain the positive frequency expression of the local light as follows:

$$\hat{\varepsilon}_1^{(+)} = \mathrm{i}\left(\frac{\hbar\omega}{2\varepsilon_0 cT}\right)^{1/2}\left[\sqrt{N_1}\left(ru_{n-1}(x) + t\,\mathrm{e}^{\mathrm{i}\phi}u_{n+1}(x)\right) + \sum_m \delta\hat{a}_{m1}\cdot u_m(x)\right]. \tag{8}$$

Then we can obtain the SNR and the minimum measurable frequency shift $\Delta\omega_{\min}^{\mathrm{BHD}}$ of the balanced homodyne detection at this time. For the case of $g = 0$ and $r = 0$

$$\begin{aligned}\mathrm{SNR} &= \frac{\left(2d\sqrt{\eta N_2}\left(r\sqrt{n} - t\cos\phi\sqrt{n+1}\right)\right)^2}{w_0^2} \\ &\le \frac{\left(2d\sqrt{\eta N_2}\sqrt{2n+1}\right)^2}{w_0^2},\end{aligned} \tag{9}$$

$$\begin{aligned}\Delta\omega_{\min}^{\mathrm{BHD}} &= \frac{Dw_0}{2\left(r\sqrt{n} - t\cos\phi\sqrt{n+1}\right)\sqrt{\eta N_2}} \\ &\ge \frac{Dw_0}{2\sqrt{2n+1}\sqrt{\eta N_2}}.\end{aligned} \tag{10}$$

It can be seen from the above formula that when $\phi = \pi + 2k\pi$ and $r/t = \sqrt{n}/\sqrt{n+1}$, the SNR of the system reaches its maximum and the measurement precision arrives at its maximum. Figure 4 describes the influences of the energy weight ratio of the $(n-1)$-mode to $(n+1)$-mode on the measurement precision for different values of n.

Figure 4 shows the error function of signal light at different orders ($n = 0$, 1, 2, and 3). In particular, when $n = 0$, a minimum error is obtained at $r/t = 0$, *i.e.*, $u_{n+1}(x)$ is the best mode of the local light at this time.

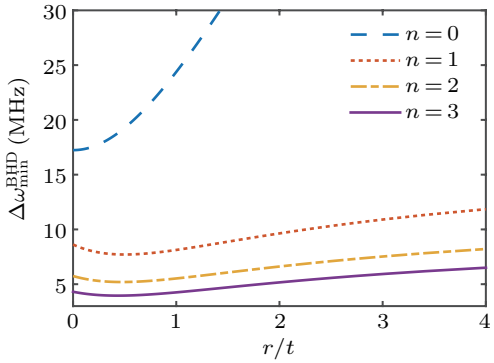


Fig. 4. Curves of minimum measurable frequency shift $\Delta\omega_{\min}^{\mathrm{BHD}}$ *versus* energy weight ratio r/t of $(n-1)$-order mode to $(n+1)$-order mode for different values of n. When $r/t = \sqrt{n}/\sqrt{n+1}$, the SNR of the system reaches maximum, and the measurement error is the smallest at this time.

3.3. Influence of modes of squeezed vacuum state on measurement precision

In addition to the mode of the local light affecting the measurement precision of the system, the mode of the squeezed vacuum state affects the measurement precision of the system. After the local light adopts the best superposition mode, the squeezed vacuum state should also adopt the mode corresponding to the local light. At this time, the photon number difference operator is

$$\hat{n}_- = \sqrt{N_1}\left(2\sqrt{2n+1}\sqrt{\eta N_2}\frac{d}{w_0} + \delta\hat{X}_2^+\right), \tag{11}$$

where $\delta\hat{X}_2^+ = \sqrt{n/(2n+1)}\delta\hat{X}_{n-1}^+ - \sqrt{(n+1)/(2n+1)}\delta\hat{X}_{n+1}^+$, $\delta\hat{X}_{n-1}^+$ and $\delta\hat{X}_{n+1}^+$ are the quadrature component fluctuation of $(n-1)$-order mode and $(n+1)$-order mode, respectively. After squeezed vacuum state is injected, the SNR and the measurement error of the frequency shift are separately

$$\begin{aligned}\mathrm{SNR} &= \frac{\left(2d\sqrt{\eta N_2}\sqrt{2n+1}\right)^2}{w_0^2} \\ &\quad\times\left(\frac{n}{2n+1}\mathrm{e}^{2r_1} + \frac{n+1}{2n+1}\mathrm{e}^{2r_2}\right),\end{aligned} \tag{12}$$

$$\Delta\omega_{\min}^{\mathrm{BHD}} = \frac{Dw_0}{2\sqrt{2n+1}\sqrt{\eta N_2}}\Big/\sqrt{\frac{n}{2n+1}\mathrm{e}^{2r_1} + \frac{n+1}{2n+1}\mathrm{e}^{2r_2}}. \tag{13}$$

In the above formulas, r_1 and r_2 are the squeezed degrees of squeezed vacuum state in $(n-1)$-order mode and $(n+1)$-order mode, respectively. Therefore, if the measurement precision is required to be higher, the squeezed vacuum state must adopt the same superposition mode as the local light, and r_1, $r_2 > 0$ must be satisfied. The influences of squeezed degrees of $(n-1)$-order mode and $(n+1)$-order mode on the SNR and measurement precision of the system are shown in Fig. 5. It can be seen from Fig. 5(a) that when the squeezed vacuum state has squeezed degrees in both the $(n-1)$-order mode and $(n+1)$-order mode, the measurement precision of the system will reach a maximum value. In particular, when the signal

light is in the 0-order mode, the measurement precision at this time loses its dependence on the squeezed factor r_1. The reason is that the coefficient before r_1 in Eq. (13) is 0, so the precision at this time will increase with r_2 increasing. Figure 5(b) shows that with the increase of the squeezed factors r_1, r_2, and the mode order of signal light, the Doppler measurement precision increase. Simulation related parameters are signal light power $P_s = 0.08$ W and loss rate $\eta = 96\%$.

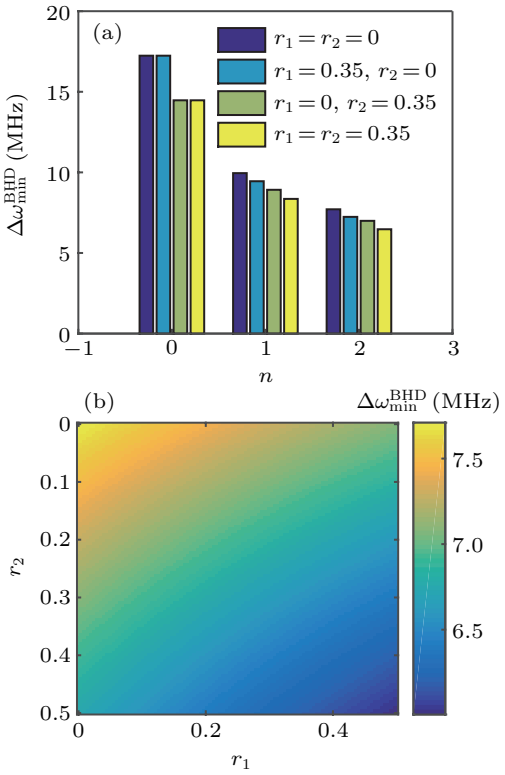


Fig. 5. (a) Influences of mode of squeezed vacuum state on precision for different orders of signal light, showing that when the squeezed vacuum state in both $(n-1)$-order mode and $(n+1)$-order mode is injected, the measurement precision of our system reaches a maximum value. (b) Influence of squeezed factors r_1 and r_2 on measurement precision for mode order of signal light $n = 2$, showing that with the increase of r_1 and r_2, the measurement error of the system decreases.

When $r_1 = r_2 = r$, comparing Eq. (13) with Eq. (6), we can find that after we adopt the superposition mode of the local light and the squeezed vacuum state injection, the measurement precision of Doppler frequency shift is improved by $\sqrt{(2n+1)/(n+1)}$ times, with other parameters unchanged, parametric amplification factor $g = 0$.

4. Conclusions and perspectives

In this paper, proposed is a tiny Doppler frequency shift precision measurement scheme, in which the high-order mode signal light is used to improve the measurement precision of Doppler frequency shifts. At the same time, a parametric amplification process and squeezed vacuum state are taken into account in the system, and the Cramér–Rao bound of the coherent light detection is broken through. For the signal light in the Gaussian mode, when the amplification factor $g = 1$ and the squeezed factor $r = 0.5$, the measurement error of Doppler frequency shift is 14.4% of the Cramér–Rao bound of coherent light. The measurement precision of Doppler frequency shift can be improved when an n-order ($n > 0$) Hermite–Gaussian beam is adopted as the signal light. At this time, when the local light and the squeezed vacuum state are in the best superposition mode, the measurement precision is further improved by $\sqrt{(2n+1)/(n+1)}$ times.

Appendix A

In Appendix A, the relevant theoretical formulas about balanced homodyne detection are given. According to the Eq. (B1) in Appendix B, we can give the expression of the positive frequency part of the local light and the signal light as follows:

$$\hat{\varepsilon}_{\mathrm{Lo}}^{(+)}(x) = \mathrm{i}\left(\frac{\hbar\omega}{2\varepsilon_0 cT}\right)^{1/2}\sum_n \hat{a}_n u_n(x), \tag{A1}$$

$$\hat{\varepsilon}^{(+)}(x) = \mathrm{i}\left(\frac{\hbar\omega}{2\varepsilon_0 cT}\right)^{1/2}\sum_n \hat{a}_n u_n(x). \tag{A2}$$

After the two input fields interfere with the 50:50 beam splitter, the positive frequency expressions of the two output fields are expressed as

$$\hat{\varepsilon}_1^{(+)} = 1/\sqrt{2}\left(\hat{\varepsilon}_{\mathrm{Lo}}^{(+)} + \hat{\varepsilon}^{(+)}\right), \tag{A3}$$

$$\hat{\varepsilon}_2^{(+)} = 1/\sqrt{2}\left(\hat{\varepsilon}^{(+)} - \hat{\varepsilon}_{\mathrm{Lo}}^{(+)}\right). \tag{A4}$$

Then the difference between the photocurrents of the two detectors is

$$\begin{aligned}\hat{n} = \hat{n}_1 - \hat{n}_2 &= \int_{-\infty}^{+\infty}\hat{\varepsilon}_1^{(+)+}\hat{\varepsilon}_1^{(+)}\mathrm{d}x - \int_{-\infty}^{+\infty}\hat{\varepsilon}_2^{(+)+}\hat{\varepsilon}_2^{(+)}\mathrm{d}x \\ &= \frac{\hbar\omega_0}{2\varepsilon_0 cT}\sum_{n=0}^{\infty}\left[\hat{a}_n^{+}\hat{a}_{\mathrm{Lo},n} + \hat{a}_{\mathrm{Lo},n}^{+}\hat{a}_n\right].\end{aligned} \tag{A5}$$

Since the intensity of the local light is much greater than that of signal light, we linearize the operator $\hat{a}_{\mathrm{Lo},n}$ in the above equation to obtain the formula $\hat{a}_{\mathrm{Lo},n} = \sqrt{N_1}\,\mathrm{e}^{\mathrm{i}[(\omega_1-\omega_2)t+\phi_0]}$, where $\sqrt{N_1}$ is the photon number of the local light in the detection time T, and $(\omega_1 - \omega_2)t + \phi_0$ is the phase difference between signal light and local light. At the moment t, N_2 is the number of photons in the signal light and satisfies $N_2 \ll N_1$. After ignoring high-order small items, we can obtain

$$\begin{aligned}\hat{n}_- = {} & 2\sqrt{N_1 N_2}\cos\left((\omega_1 - \omega_2 \pm \Delta\omega)t + \phi_0\right) \\ & + \sqrt{N_1}\delta\hat{X}_2^{+}.\end{aligned} \tag{A6}$$

Appendix B

In this section, the quantum theory of electromagnetic field and related theoretical derivation of balanced homodyne detection are given. The electromagnetic field can be expanded by using a set of orthogonal mode basis vectors. The

expression of the positive frequency part of the electromagnetic field is

$$\hat{\varepsilon}^{(+)}(x) = \mathrm{i}\left(\frac{\hbar\omega}{2\varepsilon_0 cT}\right)^{1/2}\sum_n \hat{a}_n u_n(x). \tag{B1}$$

In the above formula, ω is the angular frequency of the electromagnetic field, c is the speed of light, T is the detection integration time, ε_0 is the permittivity of free space, $\hat{a}_n$ is the annihilation operator of the n-order mode, and $u_n(x)$ is the n-order Hermite–Gaussian mode.

The annihilation operator $\hat{a} = \langle\hat{a}\rangle + \delta\hat{a}$ is linerarized, and only the average value of the n-order Hermite–Gaussian mode is not 0. For the signal light with a transversal displacement d, the positive frequency part of the light field can be written as

$$\hat{\varepsilon}^{(+)}(x) = \mathrm{i}\left(\frac{\hbar\omega}{2\varepsilon_0 cT}\right)^{1/2}\left(\sqrt{N}u_n(x+d) + \sum_n u_n(x)\delta\hat{a}_n\right). \tag{B2}$$

Since the transversal displacement d is small, satisfying $d \ll w_0$, where w_0 is the beam waist radius, the signal light can be expanded into a Taylor series, and with retaining the first-order term, the following expression is obtained:

$$u_n(x+d) \approx u_n(x) + u_n'(x)\,d. \tag{B3}$$

Here, $u_n'(x) = \left(\sqrt{n}u_{n-1}(x) - \sqrt{n+1}u_{n+1}(x)\right)/w_0$. It can be seen that the first derivative of the n-order mode is the superposition mode of the $(n-1)$-order mode and the $(n+1)$-order mode. When the n-order mode is adopted as the signal light, the local light needs to adopt the $(n+1)$-order mode in order to obtain the transversal displacement d of the signal light. The expression of positive frequency part of the local light and that of signal light are respectively as follows:

$$\hat{\varepsilon}_1^{(+)} = \mathrm{i}\left(\frac{\hbar\omega}{2\varepsilon_0 cT}\right)^{1/2}\left[\frac{\sqrt{N_1}}{\sqrt{2n+1}}\sqrt{n+1}u_{n+1}(x) + \sum_m \delta\hat{a}_{m1}\cdot u_m(x)\right], \tag{B4}$$

$$\hat{\varepsilon}_2^{(+)} = \mathrm{i}\left(\frac{\hbar\omega}{2\varepsilon_0 cT}\right)^{1/2}\left[\sqrt{\eta N_2\cosh^2 g} \times\left(u_n(x) + \frac{d}{w_0}\left(\sqrt{n}u_{n-1}(x) - \sqrt{n+1}u_{n+1}(x)\right)\right) + \sum_m \delta\hat{a}_{2m}\cdot u_{2m}(x)\right]. \tag{B5}$$

Appendix C

In this section, the theoretical derivation of the quantum Cramér–Rao bound of coherent light measurement is presented.[24] For the coherent light with a transversal displacement d, the photon number distribution at coordinate x obeys the Poisson distribution:

$$P(x,d) = \frac{\bar{n}(x,d)^{n(x)}}{n(x)!}\mathrm{e}^{-\bar{n}(x,d)}. \tag{C1}$$

Then the logarithm likelihood function at coordinate x can be defined as

$$\ln[P(x,d)] = n(x)\ln[\bar{n}(x,d)] - \bar{n}(x,d) - \ln[n(x)!]. \tag{C2}$$

According to Eq. (C2), we can obtain the first-order derivative S of the logarithm likelihood function:

$$S = \left.\frac{\partial\ln[P(x,d)]}{\partial d}\right|_{d=0} = n(x)\cdot\frac{\bar{n}'(x,d)}{\bar{n}(x,d)} - \bar{n}'(x,d), \tag{C3}$$

where $\bar{n}'(x,d) = \partial\bar{n}(x,d)/\partial d$.

In order to obtain the Fisher information expression, the variance of S is required, and we can obtain the following equation by combining Eq. (C1) with Eq. (C3):

$$E\left(S^2\right) = \sum_{n=0}^{\infty} S^2\cdot\frac{\bar{n}(x,d)^{n(x)}}{n(x)!}\mathrm{e}^{-\bar{n}(x,d)} = \frac{\bar{n}'(x,d)^2}{\bar{n}(x,d)}, \tag{C4}$$

$$E(S) = \sum_{n=0}^{\infty}\left[n(x)\cdot\frac{\bar{n}'(x,d)}{\bar{n}(x,d)} - \bar{n}'(x,d)\right] \times\frac{\bar{n}(x,d)^{n(x)}}{n(x)!}\mathrm{e}^{-\bar{n}(x,d)} = 0. \tag{C5}$$

Then we can obtain the Fisher information expression

$$I_{\mathrm{F}} = E\left(S^2\right) - E(S)^2 = \bar{n}'(x,d)^2/\bar{n}(x,d).$$

For a high-order Hermite–Gaussian beam with a transversal displacement d, the average number of photons at coordinate x satisfies $\bar{n}(x,d) = N_2 u_n^2(x,d)$, where N_2 is the photon number of the signal beam, and $u_n(x,d)$ is a amplitude expression of a TEM_{n0} mode.

From this we can obtain the Fisher information expression at coordinate x as follows:

$$I_{\mathrm{F}}(x) = 4N_2\left[\frac{\sqrt{n}}{w_0}u_{n-1}(x) - \frac{\sqrt{n+1}}{w_0}u_{n+1}(x)\right]^2. \tag{C6}$$

After integrating Eq. (C6) with espect to coordinate x, the Fisher information expression of the entire transversal distribution of the signal light is obtained and given below:

$$I_{\mathrm{F}} = \int_{-\infty}^{+\infty}\mathrm{d}x I_{\mathrm{F}}(x) = 4N_2(2n+1)/w_0^2. \tag{C7}$$

Then the error lower limit of the transversal displacement d (or the minimum measurable displacement $d_{\min}$) is

$$d_{\min} = \frac{w_0}{2\sqrt{2n+1}\sqrt{N_2}}. \tag{C8}$$

The minimum measurable frequency shift of coherent light (or called $\Delta\omega_{\mathrm{CRB}}$) is obtained from the equation $d_{\min} = \Delta\omega_{\min}/D$ as follows:

$$\Delta\omega_{\mathrm{CRB}} = D\cdot\frac{w_0}{2\sqrt{2n+1}\sqrt{N_2}}. \tag{C9}$$

It is worth mentioning that the calculation of the quantum Cramér–Rao bound does not depend on the specific measurement. It can be used as a standard to evaluate the quality of measurements. The closer to the quantum Cramér–Rao bound the variance of the measurement is, the better the evaluation will be.

References

[1] Brousseau C, Mahdjoubi K and Emile O 2019 *Electron. Lett.* **55** 709
[2] Zhuo H, Wen A J and Tu Z Y 2020 *Opt. Commun.* **470** 125798
[3] Yang V, Gordon M, Qi B, *et al.* 2003 *Opt. Express* **11** 794
[4] Lieb K P, Börner H G, Dewey M S, *et al.* 2016 *Phys. Lett. B* **215** 50
[5] Liu F, Zhou Y, Yu J, Guo J, Wu Y, Xiao S, Wei D, Zhang Y, Jia X and Xiao M 2017 *Appl. Phys. Lett.* **110** 021106
[6] Ono T and Hofmann H F 2010 *Phys. Rev. A* **81** 033819
[7] Berry D W, Hall M J W and Wiseman H M 2013 *Phys. Rev. Lett.* **111** 113601
[8] Du W, Jia J, Chen J F, Ou Z Y and Zhang W 2018 *Opt. Lett.* **43** 1051
[9] Ou Z Y 2012 *Phys. Rev. A* **85** 023815
[10] Manceau M, Leuchs G, Khalili F and Chekhova M 2017 *Phys. Rev. Lett.* **119** 223604
[11] Hosten O and Kwiat P 2008 *Science* **319** 787
[12] Pfeifer M and Fischer P 2011 *Opt. Express* **19** 16508
[13] Delaubert V, Treps N, Lassen M, Harb C C, Fabre C, Lam P K and Bachor H A 2006 *Phys. Rev. A* **74** 53823
[14] McKenzie K, Shaddock D A, McClelland D E, Buchler B C and Lam P K 2002 *Phys. Rev. Lett.* **88** 231102
[15] Abadie J, Abbott B, Abbott R, *et al.* 2011 *Nat. Phys.* **7** 962
[16] Shao C G, Chen Y F, Sun R, Cao L S, Zhou M K, Hu Z K, Yu C and Miiller H 2018 *Phys. Rev. D* **97** 024019
[17] Otterstrom N, Pooser R C and Lawrie B J 2014 *Opt. Lett.* **39** 6533
[18] Fabre C, Fouet J B, and Maitre A 2000 *Opt. Lett.* **25** 76
[19] Treps N, Grosse N, Bowen P, Fabre C, Bachor H A and Lam P K 2003 *Science* **301** 940
[20] Hsu M T L, Delaubert V, Lam P K and Bowen W P 2004 *J. Opt. B Quantum Semiclassical Opt.* **6** 495
[21] Delaubert V, Treps N, Lassen M, Harb C C, Fabre C, Lam P K and Bachor H A 2006 *Phys. Rev. A* **74** 053823
[22] Viza G I, Martínez-Rincón J, Howland G A, *et al.* 2013 *Opt. Lett.* **38** 2949
[23] Starling D J, Dixon P B, Jordan A N, *et al.* 2010 *Phys. Rev. A* **82** 063822
[24] Pinel O, Fade J, Braun D, *et al.* 2012 *Phys. Rev. A* **85** 010101(R)